

BUCKLING OF THIN-WALLED SILOS AND TANKS UNDER AXIAL LOAD—SOME NEW ASPECTS

By Martin Pircher¹ and Russell Q. Bridge²

ABSTRACT: The strength of thin-walled cylindrical shell structures is highly dependent on the nature and magnitude of imperfections. Most importantly, circumferential imperfections have been reported to have an especially detrimental effect on the buckling resistance of these shells under axial load. Due to the manufacturing techniques commonly used during the erection of steel silos and tanks, specific types of imperfections are introduced into these structures, among them circumferential weld-induced imperfections between strakes of steel plates. A study on several factors influencing the buckling of silos and tanks was carried out using the finite-element method. The interaction between neighboring circumferential weld imperfections was investigated, and it was found that the influence on the buckling behavior depended on the strake height in relation to the linear meridional bending half-wavelength and the depth of the imperfection. The shape of localized circumferential weld imperfections was found to influence the buckling behavior of silos and tanks. The influence of a recently developed shape function on the buckling behavior has been examined. The strengthening effect of weld-induced residual stress fields was also studied, and the extent of the increase in buckling strength was derived for a large range of cylinder geometries.

INTRODUCTION

Storage bins are an important link in the chain of materials handling for a large number of industries. In many cases, the ability of storage facilities to provide a reliable flow of bulk material determines the success of a plant. Many such storage bins are manufactured from steel plates and thus belong to the group of thin-walled shell structures that are renowned for their “imperfection-sensitive behavior.” Small deviations from the nominal or perfect geometry result in significant loss of strength of such structures, where imperfections of just one wall thickness in magnitude can reduce the axial buckling stress to only one-third the classical value for perfect cylinders (Koiter 1945).

Steel silos and tanks are constructed from plates that are rolled to the correct curvature and welded together to form strakes. Several strakes of curved plates, placed on top of each other then form the completed structure (Fig. 1). At each circumferential weld, a slight hourglass depression occurs forming axisymmetric imperfections that are known to be most deleterious.

While classical theory works well to predict the stability of flat plates and columns, the situation for circular cylindrical shells is quite different. Taking all the usual simplifications of classical theory into account, the following can be observed as illustrated in Fig. 2. All three of these systems show a linear response until a critical load is reached. Idealized columns cannot develop transverse stresses to restrain out-of-plane displacements. The response after buckling is therefore undefined. Imperfections cause increased lateral displacements, and the maximum load is reached asymptotically. The load capacity of flat plates increases even after the critical load has been reached as transverse tensile stresses work against the growth of out-of-plane displacements. Again, the postbuckling response of the perfect plate is approached asymptotically by an imperfect plate, smoothing the kink in the load-deflection curve. The postbuckling response of a perfect cylinder is sig-

nificantly different. A steep descent in the characteristic can be observed after the critical load has been reached. Imperfections can reduce the buckling strength dramatically as the narrow gap between the prebuckling and the postbuckling segments of the response curve is bridged at a much lower level.

Plasticity affects the behavior of the three member systems in similar ways as the load capacity of each member drops off once elastic limits are exceeded. The severest reductions in strength occur when the yield limit and the critical buckling load are close to each other.

Calladine (1995) lists three criteria to define imperfection-sensitive behavior:

- Buckling loads that fall short of the predictions of classical buckling theory
- Unpredictability of buckling strength, as evidenced by the wide scatter of experimentally observed buckling loads

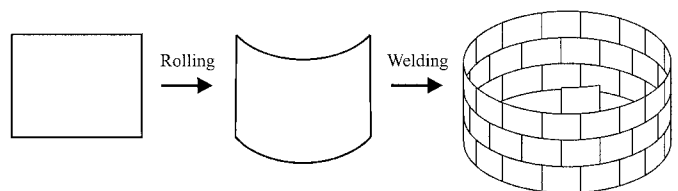


FIG. 1. Erection of Circular Silo or Tank

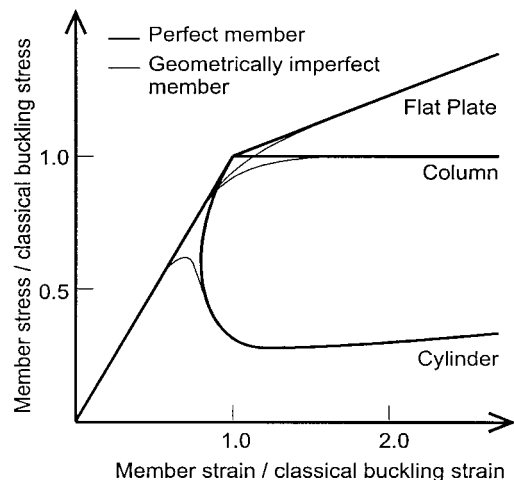


FIG. 2. Postbuckling Behavior of Elastic Flat Plates, Columns, and Cylinders

¹Prof., Univ. of Western Sydney, School of Civ. Engrg. and Envir., Sydney 2474, Australia.

²Prof., Univ. of Western Sydney, School of Engrg. and Industrial Des., Locked Bag 1797, South Penrith, New South Wales 1797, Australia.

Note. Associate Editor: Mark Bowman. Discussion open until March 1, 2002. To extend the closing date one month, a written request must be filed with the ASCE Manager of Journals. The manuscript for this paper was submitted for review and possible publication on January 3, 2001; revised May 22, 2001. This paper is part of the *Journal of Structural Engineering*, Vol. 127, No. 10, October, 2001. ©ASCE, ISSN 0733-9445/01/0010-1129-1136/\$8.00 + \$.50 per page. Paper No. 22677.

- Unstable, dynamic behavior of the shell after the maximum load has been reached—leading to catastrophic failure in some circumstances

Thin-walled circular cylindrical structures have been proven to show all of the above-mentioned behavior patterns. Buckling loads in laboratory tests are usually scattered. Very small differences in the amplitude of imperfections can lead to enormous differences in strength. Buckling typically occurs suddenly, and dynamic effects distinguish the behavior immediately after the critical load has been reached.

In Koiter's original theory (Koiter 1945) and later again in his special theory (Koiter 1963), axisymmetric imperfections in the shape of indefinitely extensive sinusoidal waves were used among other imperfection patterns to determine the imperfection sensitivity of thin-walled cylindrical shells. The fact that axisymmetric imperfections lead to the most dramatic reductions in buckling strength under axial load has been known since then but did not receive much attention as practical applications of this imperfection geometry did not exist at the time. In the late 1960s and early 1970s, the erection of ever larger silos and tanks led to a change in this attitude as these structures displayed significant axisymmetric imperfections at circumferential welds. Research by Tennyson and Muggerridge (1969), Hutchinson et al. (1971), and Amazigo and Budianski (1972) investigated localized axisymmetric imperfections and demonstrated that a single axisymmetric imperfection can still have a significant effect on the buckling strength of thin-walled cylinders. Two groundbreaking papers by Rotter and Teng (1989) and Teng and Rotter (1992) contributed more research on the topic of circumferential weld-induced imperfections using numerical methods. Until then only geometric imperfections in indefinitely long cylindrical shells were considered. Rotter (1996) did a limited study that included interaction between neighboring welds and residual stresses for a small number of examples contradicting the only other study that takes residual stresses into account (Häfner 1982).

Three aspects of axisymmetric imperfections in shell-buckling problems have been investigated, and results will be presented in this paper. First, a study on parameters of the imperfection shape was performed considering previously proposed shape functions and a newly developed shape function (Pircher et al. 2000) based on actual measurements on silos. Second, an investigation was made on the effects of interaction between neighboring weld imperfections on the buckling behavior. Third, a parametric study taking into account weld-induced residual stresses was undertaken, and results are given to document the influence of weld-induced residual stress fields on the buckling behavior.

MODEL OF CYLINDRICAL STRUCTURE

A commercially available computer program called ABAQUS (Hibitt, Karlsson & Sorensen 1998), which utilizes the finite-element (FE) method was employed for the structural modeling. Full shell elements that allow loading and displacements in all directions were used in the buckling analyses as bifurcation into nonaxisymmetric modes had to be expected.

It was assumed that the strength of the shell structure is limited by bifurcation into a nonaxisymmetric mode. Elastic-plastic material properties were considered, but buckling always took place at stress levels well below the yield level for the considered examples. The elastic properties were set to represent steel with an elastic modulus of $E = 200,000$ MPa and a Poisson's ratio of $\nu = 0.3$.

Geometric Properties

Due to restrictions in computer capacity, it was decided to use a cylindrical model of one circumferential weld and half

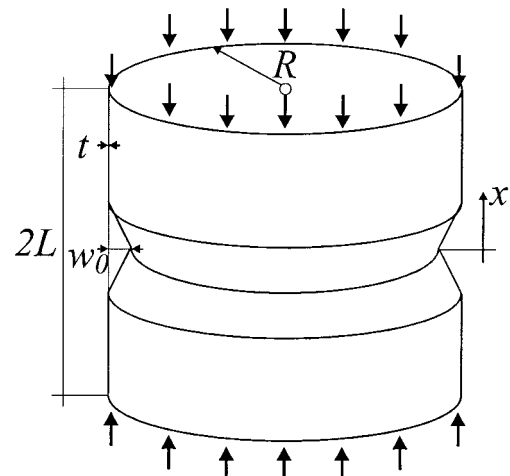


FIG. 3. Geometric Parameters of Analyzed Model

a stroke above and below this weld (Fig. 3). It was assumed that variations in the loading are small enough within this limited region to be negligible and loads were assumed to be constant within the model.

Perfectly axisymmetric cylinders under axial load are known to bifurcate into nonaxisymmetric buckling modes (Yamaki 1984) consisting of periodic waves around the circumference. Previous studies of the circumferential weld imperfection (Tennyson and Muggerridge 1969; Steinhardt and Schultz 1970; Rotter and Teng 1989; Berry et al. 2000) have shown that the buckling patterns are also symmetric about the weld. A number of different modeling techniques have been used in the past to take advantage of the periodical symmetries. The computationally most efficient simplification is a model that uses only one half-wave of one particular buckling pattern. A number of different patterns have to be examined in order to find the critical buckling mode (i.e., the buckling mode associated with the lowest load). This approach was used to derive the results presented in this paper.

A preliminary study was performed to determine the optimal element mesh for each of the studies. Forty elements in the circumferential direction and 70 elements in the axial direction were used with an especially fine mesh near the weld to accommodate the modeling of residual stresses and to accurately represent variations of shape functions in that area. Full details of the FE modeling are given in Pircher and Bridge (2000).

Shape of Weld Imperfection

Several shape functions to describe the geometry of a circumferential weld in a silo or tank have been suggested in the past (Tennyson and Muggerridge 1969; Steinhardt and Schulz 1970; White and Dwight 1977; Häfner 1982; Rotter and Teng 1989; Fritschi, unpublished paper, 1995; Rotter 1996). Most of these suggestions are based on theoretical assumptions and only a few shape functions are loosely based on actual field measurements of existing structures. A detailed discussion of all these shape functions can be found in Pircher et al. (2000). Pircher et al. (2000) also suggest a new shape function given by

$$w(x) = w_0 \cdot e^{-\pi x/\lambda} \left(\cos \frac{\pi x}{\lambda} + \zeta \cdot \sin \frac{\pi x}{\lambda} \right) \quad (1)$$

which is based on elastic shell theory and which was calibrated against measurements taken by Ding (1992) on a silo at Port Kembla, Australia. It can also be used to give a close approximation to shape functions used by other researchers.

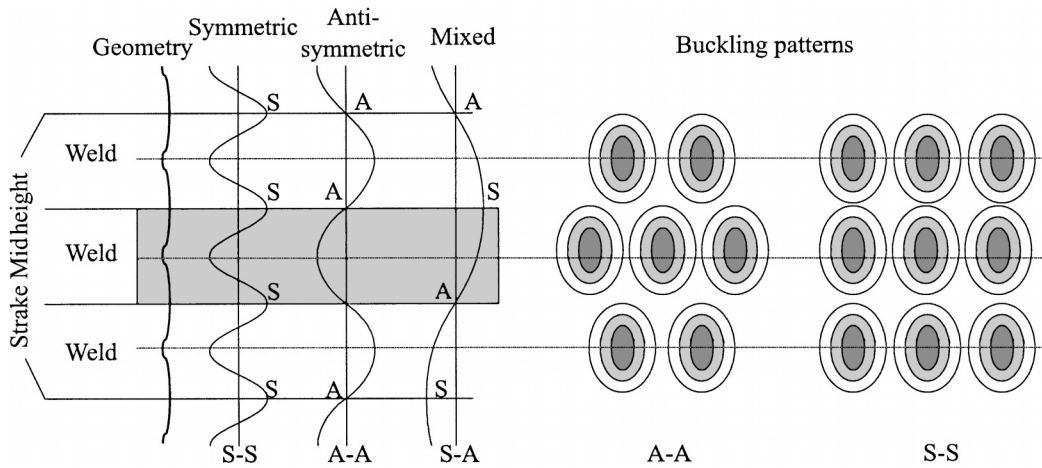


FIG. 4. Buckling Patterns and Boundary Conditions

Interaction between Neighboring Circumferential Imperfections

Strake heights in silos and tanks are dictated by the size of steel plates commercially available. This typically leads to strake heights that are too small to isolate the effects of neighboring circumferential weld imperfections from each other. Rotter (1996) proposed a system of taking the interaction between weld imperfection into account, which is based on the assumptions that neighboring imperfections are equally detrimental to the buckling strength. This assumption is rather conservative, but it allows the results to be used with confidence until better data is available. Fig. 4 illustrates possible buckling patterns and their inclusion in an FE model simply by varying the boundary conditions (symmetry and antisymmetry) at strake midheight. Looking at one meridian in the buckled mode, three combinations of boundary conditions can be defined: S-S (symmetry at strake midheight on both sides), A-A (antisymmetry at strake midheight on both sides), and A-S (symmetry at strake midheight on one side and antisymmetry on the other side) as shown in Fig. 4. Rotter (1996) found that the A-A condition yields the lowest bifurcation loads and the S-S condition the highest. Unless otherwise noted, all results presented here are under the assumption of A-A boundary conditions. A more detailed discussion of the implications and limitations of this system can be found in Pircher and Bridge (2000).

Weld-Induced Residual Stress Field

Including residual stresses into a weld imperfection of a given geometry is a requirement for a number of analyses performed for the present work. Two approaches to this problem have been proposed, although the task of modeling residual stresses in thin-walled shell structures has not been discussed widely in the literature (Häfner 1982; Holst et al. 1996; Rotter 1996). In the first approach, which has been chosen by Häfner (1982), a given pattern of residual stresses is superimposed onto the structure prior to the buckling analysis. Rotter (1996), on the other hand, argued that the residual stresses arise from a physical action (the cooling of the weld and the lack of fit between plates). This physical action was replicated in the analysis of Rotter (1996), and a pattern of residual strains was applied onto the area near the weld. This consequently led to the development of a corresponding stress field. Both strategies are valid and have their advantages and disadvantages. A thorough discussion of these two methods and a comparison of results are given in Pircher and Bridge (2000).

When a pattern of residual stresses is postulated for a struc-

tural component, this pattern must satisfy equilibrium throughout the structure. This task is comparatively simple for structures in which stresses are essentially 1D (i.e., beams, flat plates, columns, and many others). However, this is not the case in shells where stresses are 2D and affected by the curvature of the shell. Imposing a reasonable residual strain pattern effectively models the process that leads to the residual stress field in the vicinity of the circumferential weld. All components of the stress field are automatically generated as a result of the strain loading of the structure. Strain loading according to Rotter (1996) was applied inside an area of 4.2 wall thicknesses from the weld center. This area was assumed to experience a shrinkage strain equal to the yield strain. Stresses generated by the residual strain field will also lead to displacements as the structure attempts to relieve some of the ensuing stresses by deforming. These deformations have to be taken into account when modeling cylinders with specific imperfection shapes. The deformations generated by the application of residual stresses have to be subtracted from the imperfection of the initial model without residual stress so that the final model, which later includes the residual stresses, has the desired shape.

RESULTS

Influence of Weld Shape

A shape function describing a circumferential weld imperfection based on elastic shell theory [(1)] has been proposed in Pircher et al. (2000) and has been calibrated against field measurements gathered by Ding (1992). A parametric study was performed to investigate the influence of the two key parameters of this function on the buckling strength of thin-walled cylinders with a circumferential weld-induced imperfection. The two parameters in question are, first, the half-wavelength of the imperfection λ , and, second, the parameter ζ , which indicates the degree of "roundness" at the center of the weld ($\zeta = 0$ for a pointy imperfection and $\zeta = 1$ for a round shape). The study was performed at first for short cylinders with $R = 12,000$ mm, $R/t = 1,000$, and $L = 1,500$ mm $= 1.62\lambda_0$. Parameter ζ was kept constant for $\zeta = 0, 0.25, 0.5, 0.75$, and 1.0 , respectively, and the half-wavelength of the shape function λ was varied. All curves intercept at one point for $\lambda = 1.73\lambda_0$ (Fig. 5). Before this point, buckling strengths for ζ close to 0 are considerably higher than for shapes with ζ close to 1. However, for values of $\lambda > 1.73\lambda_0$, this is reversed, and shape functions with a rather pointed shape at the weld were shown to be weaker than more rounded shapes (Fig. 5). To compare these results with results given in Teng and

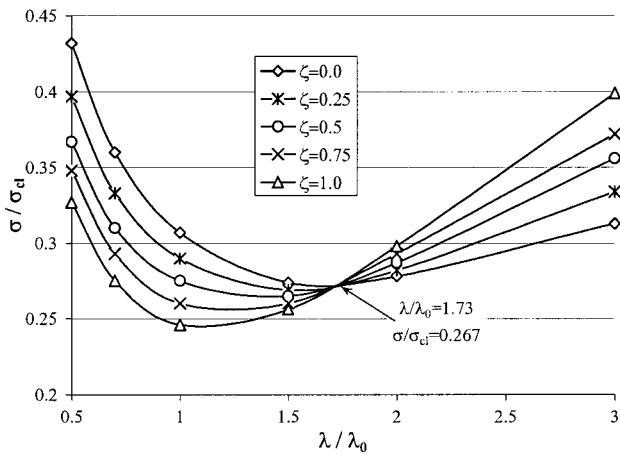


FIG. 5. Buckling Strength for Variations of λ and ζ for Short Cylinder

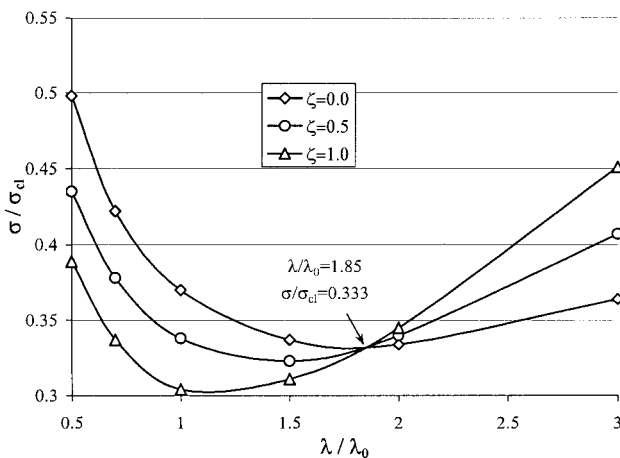


FIG. 6. Buckling Strength for Variations of λ and ζ for Long Cylinder

Rotter (1992), the same series of analyses was performed again for a “long cylinder.” Results for this second investigation are given in Fig. 6. Again, all curves intercept in one point, this time at $\lambda = 1.85\lambda_0$. The corresponding curve in Fig. 6 for $\zeta = 1$ matches the corresponding curve in Rotter and Teng (1992). The difference in buckling strength between the two extremes ($\zeta = 1$ and $\zeta = 0$) are of considerable magnitude for half-wavelengths well away from the intersection point. There is also a distinct minimum between $\lambda = 1.0\lambda_0$ and $\lambda = 2.0\lambda_0$ for all curves.

Curves for constant values of λ for variations of ζ are given in Pircher and Bridge (2000) for both the short and the long cylinders. Both diagrams clearly show a linear relationship between the buckling strength and values of ζ . Linear interpolation between buckling strengths for the two extreme values of $\zeta = 0$ and $\zeta = 1$ is therefore appropriate.

Pircher et al. (2000) give an extensive overview on shape functions proposed by other researchers. The buckling strengths for these functions for a short cylinder of $R = 12,000$ mm, $R/t = 1,000$, and $L = 1,500$ mm were determined and are given in Table 1 for the same imperfection amplitude of $w_0/t = 1.0$. Values of buckling strength were found to cover a wide range from $\sigma/\sigma_{cr} = 0.238$ to 0.470. These imperfection shapes were then approximated by the new shape function given in (1) using a least-square fit. The results of this approximation (values for λ/λ_0 and ζ) are given in Table 1. These results indicated a rather wide spread of half-wavelengths of λ/λ_0 and degree of roundness ζ . Even for the same magnitude of imperfection ($w_0/t = 1.0$) the shape of imperfection has a significant effect on the buckling strength as shown in Fig. 7.

TABLE 1. Result of Least-Square Fit Approximation of Existing Shape Functions for $w_0/t = 1.0$

Shape function	λ/λ_0	ζ	σ/σ_{cr}
Rotter and Teng (1989) B	1	0	0.302
Rotter and Teng (1989) A	1	1	0.247
Rotter (1996) final	2.4	0	0.295
Steinhardt and Schulz (1970)	0.22	1	0.470
Häfner (1982) A	0.53	1	0.308
Häfner (1982) B	0.63	0.42	0.318
Tennyson and Muggeridge (1969)	1.39	1	0.238
Rotter (1996) closed	1.25	0.97	0.251
Rotter (1996) open	3.32	1	0.297
Rotter (1996) best	1.53	1	0.252

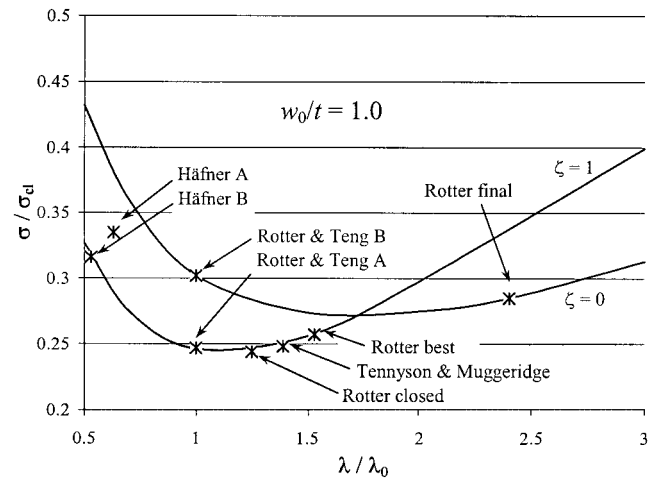


FIG. 7. Existing Shape Functions in Context of New Shape Function

Interaction between Neighboring Imperfections

A simple but efficient modeling technique to account for this interaction was proposed by Rotter (1996). Results given in Rotter (1996) and Pircher and Bridge (2000) indicate that the S-S boundary condition yields the highest buckling values and the A-A boundary condition the lowest. Boundary condition A-S lies between the two extremes but does not give symmetry at the weld—a condition observed many times in laboratory tests and failures in practice. The A-S condition was therefore not considered any further. A comparison of the A-A condition with the S-S condition over a range of strake heights and for a cylinder with an R/t -ratio of 1,000 is shown in Fig. 8. The cylinder marked as “reference silo” in Fig. 8 has the same geometric properties as the silo in Port Kembla, Australia, which was surveyed by Ding (1992) and on which much subsequent research was performed [e.g., Rotter (1996) and Pircher et al. (2000)].

Clearly, the A-A condition leads to significantly lower buckling values than the S-S conditions over the whole range of strake heights. The nature of the boundary conditions becomes insignificant for half-strake heights $L > 6,000$ mm, where both solutions equal the result for the indefinitely long cylinder. The buckling strength for the A-A boundary condition reaches a minimum between $L = 1,500$ mm and $L = 2,000$ mm. Remarkably, this is the region where most of the strakes of the reference silo at Port Kembla are situated. In the following, only the A-A boundary condition will be considered.

Various R/t -Ratios

A series of buckling analyses of FE models for four different R/t -ratios ($R/t = 500, 1,000, 1,500,$ and $2,000$ with $R = 12,000$ mm) was performed over a large range of half-strake heights. The shape of the imperfection was modeled after (1) with parameters $\lambda/\lambda_0 = 1.73$ and $\zeta = 1.0$. Results for the anal-

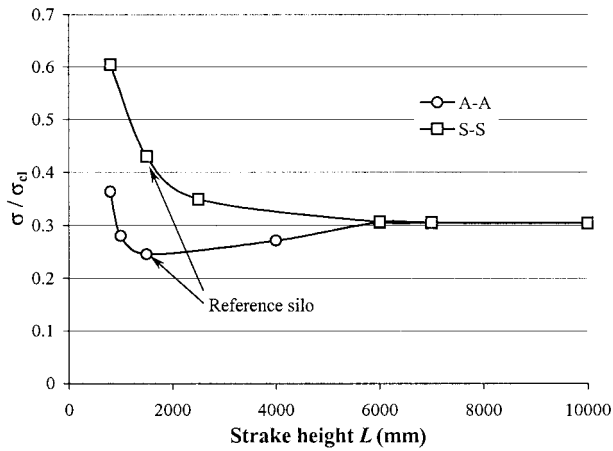


FIG. 8. Buckling Strength of A-A and S-S Boundary Conditions and Various Half-Strake Heights L

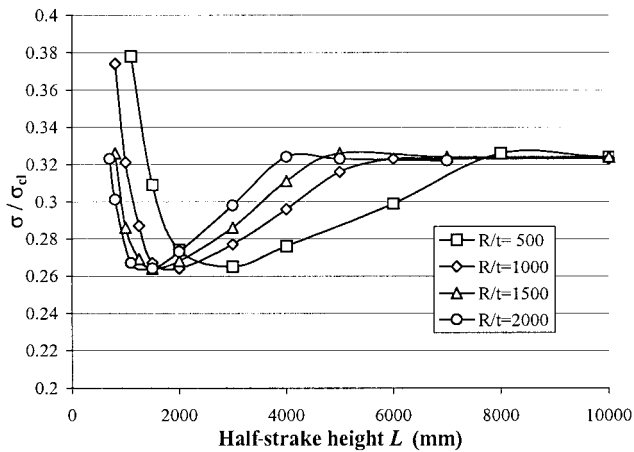


FIG. 9. Buckling Strength for Various R/t -Ratios and Half-Strake Heights L

yses for an imperfection amplitude of $w_0/t = 1.0$ are given in Fig. 9.

A perfect thin-walled cylinder buckles in a chessboard type of pattern, and the A-A condition leads to similar buckling patterns (Fig. 4). It comes as no surprise that this particular boundary condition results in a minimum in buckling strength where the buckling pattern induced by the A-A boundary condition comes closest to the chessboard pattern of the perfect cylinder. When the half-strake height becomes too short, the structure is forced to buckle into modes with more and more circumferential buckles, and the buckling strength rises again. However, it can be safely assumed, that once it rises above a certain limit, the A-A boundary condition will be replaced by different patterns. Longer half-strake heights also cause an increase in buckling resistance, eventually reaching the buckling strength of the long cylinder where boundary conditions cease to have an influence on the buckling strength of the structure.

When the results in Fig. 9 for a constant value of $w_0/t = 1.0$ are plotted as normalized against the elastic meridional half-bending wavelength λ_0 , all results were found to fall into one single curve. In another series of bifurcation analyses, other imperfection amplitudes were introduced into the FE model. Results for amplitudes of $w_0/t = 0.5, 1.0,$ and 1.5 are given in Fig. 10, normalized against the buckling strength of the long cylinder σ_{long} . Fig. 11 gives the buckling strength for imperfection amplitudes $w_0/t < 4.0$ for long cylinders. The combination of Figs. 10 and 11 can be used to determine the buckling strength σ/σ_{cl} for a wide range of half-strake heights L and imperfection amplitudes w_0/t . The difference in the choice of the shape function explains the slight difference be-

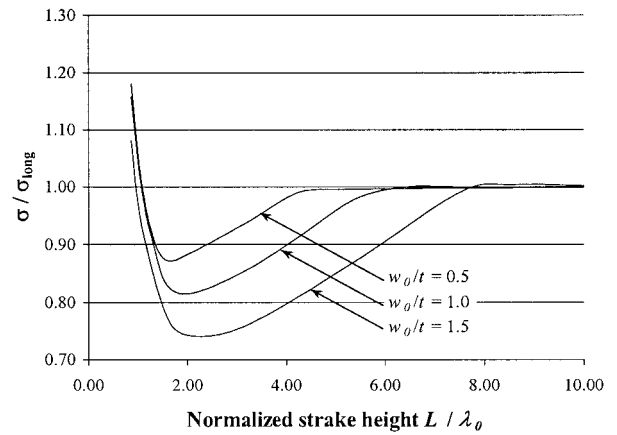


FIG. 10. Buckling Strength for Various Imperfection Amplitudes w_0/t and Half-Strake Heights L in Relation to σ_{long}

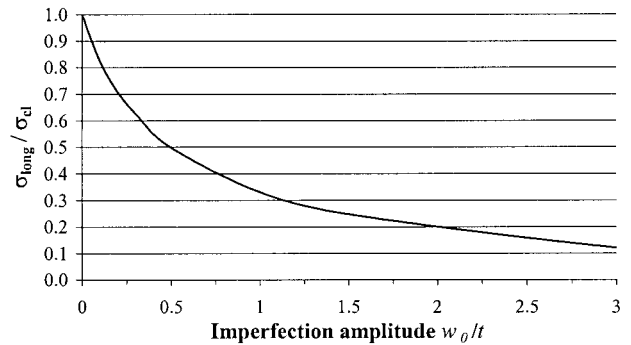


FIG. 11. Variation in Buckling Strength for Different Imperfection Amplitudes

tween the diagram given in Fig. 11 and a similar diagram given in Rotter and Teng (1989).

Weld-Induced Residual Stresses

General Influence on Buckling Behavior

Two papers are known to have discussed the effects of residual stresses at circumferential welds on the buckling behavior of thin-walled cylindrical shell structures (Häfner 1982; Rotter 1996). These two papers reach different conclusions. Häfner (1982) reported a decrease of the buckling strength of their model by up to 10%, while Rotter (1996) concluded that "Circumferential residual stresses in the welded joint, developed by shrinkage of the weld, appear to increase the buckling strength. . . ." Holst et al. (1996) cast doubt on the results of Häfner (1982) by pointing out that equilibrium was not satisfied for an unloaded shell. Ravn-Jensen and Tvergaard (1987) investigated this effect in longitudinal welds. A thorough discussion of the different modeling approaches is given in Pircher and Bridge (2000). This confirmed the findings of Rotter (1996) showing an increase—to different degrees—in buckling strength due to the presence of a residual stress field.

Circumferential membrane stresses are by far the most influential component of the stress field induced during the welding process, and the development of these stresses during the application of axial loading is shown along one meridian in Fig. 12. As axial load is applied on the initially stress-free model, circumferential compressive stresses develop near the center of the weld, thus creating an area of 2D compression. When the applied axial load approaches bifurcation load, infinitesimally small buckles start to form, which subsequently cause buckling of the structure. Circumferential compressive stresses accelerate the development of these prebuckling deformations as is shown in Fig. 13(a) (Esslinger 1967).

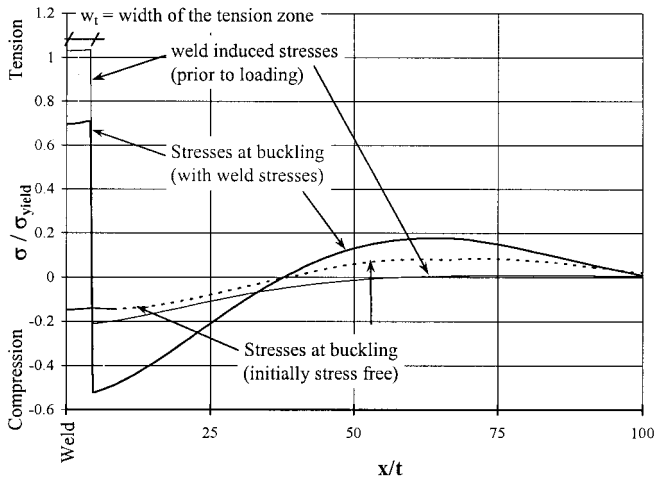


FIG. 12. Circumferential Membrane Stresses

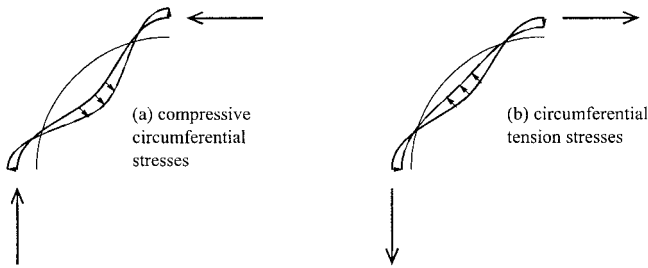


FIG. 13. Effect of Circumferential Residual Stresses

In a welded cylinder, circumferential residual stresses reach yield level in tension at the center of the weld, and even at the point of buckling under axial stress, this area is still under considerable tension (Fig. 12). Compressive residual stresses farther away from the weld typically range from 0.2 to 0.4 of the yield stress and are further increased by axial compression. The stabilizing effect of the tension stresses near the weld is illustrated in Fig. 13(b). With the increase in axial load, the tensile stresses decrease, and the compressive stresses farther away from the weld are further increased until a point is reached where the structure buckles. The second contributing factor is the presence of axial stresses and the resulting bending moments. These bending moments can be expected to become relatively more influential in more thick-walled shells and erode the stabilizing effect of the circumferential membrane stresses.

Residual tensile stresses at the weld typically reach yield level. The yield stress of the weld metal, which is deposited between two adjoining plates, is usually higher than the yield stress of the rest of the structures. This consequently leads to residual stress peaks at the weld. This effect was taken into account during a series of analyses where material properties were set in such a way that residual stresses locally at the weld reached up to four times the yield stress of the surrounding structure. The width of this strip was varied from extremely thin to about one wall thickness. The buckling strength using these FE models was found to be practically unchanged by these variations (Pircher and Bridge 2000).

Different R/t -Ratios

The two competing effects of residual stresses—the strengthening tension band of the circumferential residual membrane stresses on the one hand and the weakening effects of axial bending caused by residual stresses in the axial direction on the other hand—can be expected to lead to different degrees of influence on the buckling strength of cylinders with

different R/t -ratios. An extensive study was undertaken to investigate this influence including cylinders with R/t -ratios between 500 and 2,000 for a cylinder with $R = 12,000$ mm. The half-strike height was kept to $L = 1,500$ mm and the imperfection amplitude to $w_0/t = 1.0$.

The bifurcation stress for the critical modes is plotted in Fig. 14, first, for an FE model of a cylinder including a residual stress field, and, second, for a cylinder of exactly the same geometry but initially stress-free. At first sight, the lower curve in Fig. 14 seems to contradict the curve given in Rotter and Teng (1989) for long cylinders. However, this is not the case as the curves given in Fig. 14 also include the effects of the chosen half-strike height $L = 1,500$ mm (Fig. 10). Buckling strengths for the long cylinder ($L/\lambda_0 > 8$) proved to be constant for all R/t -ratios and almost exactly matched the diagram given in Rotter and Teng (1989). The remaining small differences could be explained by the fact that a different shape function for the imperfection geometry was used. The maximum gain for a cylinder with $R/t = 2,000$ is shown to be just under 7% of σ_{cr} . This is a considerable increase since the buckling strength of the stress-free cylinder was found to be at just over 25% of σ_{cr} .

Pircher and Bridge (2000) give detailed results for a number of bifurcation modes in addition to the critical mode for each R/t -ratio considered in this investigation. The number of bifurcation modes in close proximity to the critical mode increases considerably for higher values of R/t . It was also shown that the difference in strength between initially stress-free models and models including residual stresses becomes slightly smaller for bifurcation modes smaller than the critical mode, and this gap was found to open up slightly for modes

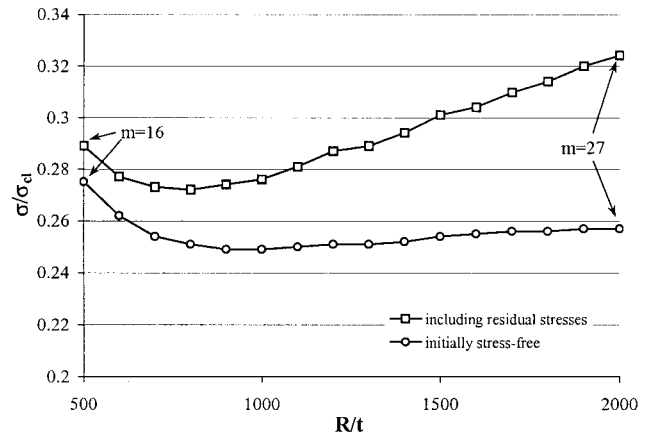


FIG. 14. Bifurcation Stress for Critical Modes for Different R/t -Ratios

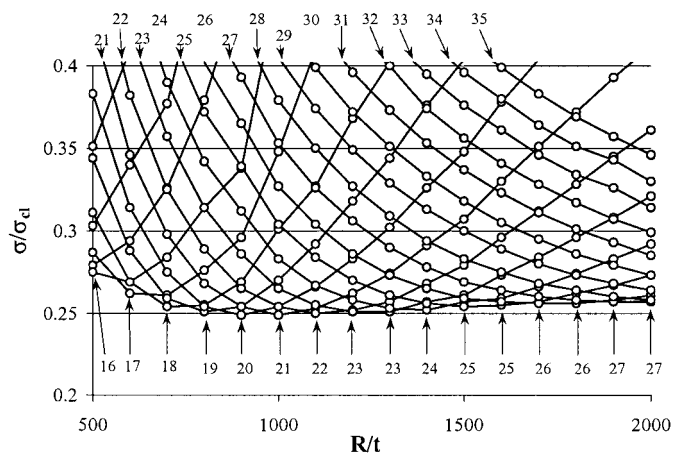


FIG. 15. Bifurcation Stresses for Various Bifurcation Modes for Initially Stress-Free Cylinders

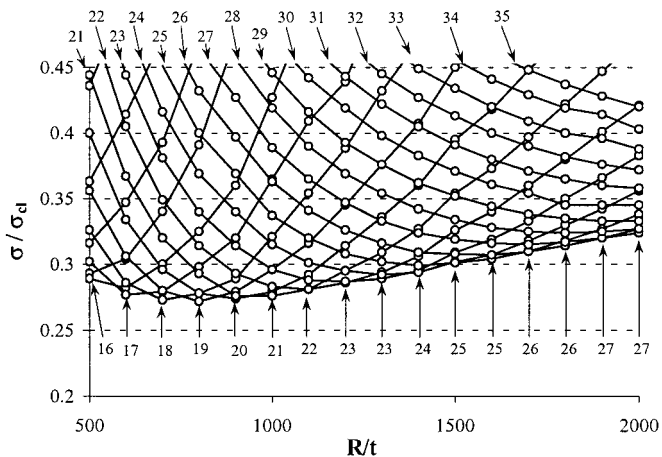


FIG. 16. Bifurcation Stresses for Various Bifurcation Modes Including Effects of Weld-Induced Residual Stresses

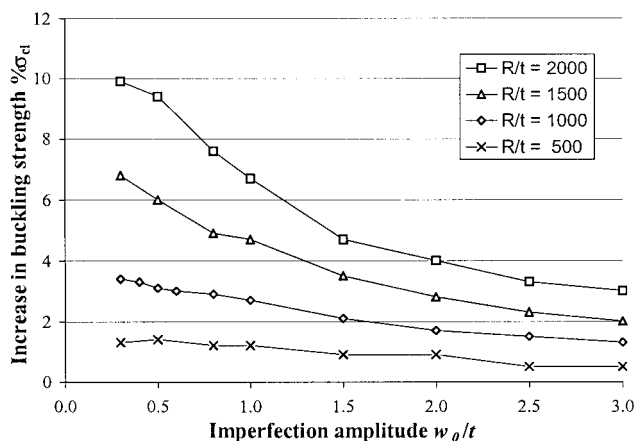


FIG. 17. Influence of Residual Stresses for Various Imperfection Amplitudes w_0/t

greater than the critical mode. These results have been used to produce the diagrams given in Figs. 15 and 16. The lower envelopes of these results (i.e., the critical modes) are those shown in Fig. 14. The diagrams in Figs. 15 and 16 give an indication of how the curves for given bifurcation modes flatten out for increased values of R/t to result in clusters of buckling modes in the close vicinity of the critical mode (lowest value of σ/σ_d).

Imperfection Amplitude

The influence of the imperfection amplitude in combination with weld-induced circumferential residual stress fields was investigated for cylinders of a half-strake height of $L = 1,500$ mm, $R = 12,000$ mm, and various R/t -ratios (500, 1,000, 1,500, and 2,000). The results for the four different cylinder geometries are shown in detail in Pircher and Bridge (2000). The increase in buckling strength due to the effect of the residual stress field (Fig. 17) is much greater for the more thin-walled shells (large R/t value) with small imperfections (small w_0/t value) than for thick-walled shells (small R/t value) with large imperfections (large w_0/t value). The greatest gain of almost 10% of σ_{cl} increase was recorded for small imperfection amplitudes ($w_0/t = 0.2$) in the most thin-walled shell investigated ($R/t = 2,000$). Again, this represents quite a remarkable increase in the buckling strength for shells of such a high slenderness.

CONCLUSIONS

Three aspects regarding the buckling of thin-walled cylindrical shell structures with circumferential weld-induced im-

perfections have been investigated: the influence of the shape of the weld on the buckling behavior; the interaction between neighboring weld imperfections; and the influence of weld-induced residual stress fields on the buckling behavior. Parameter studies were performed to study these problems for a range of cylinder geometries. The following conclusions can be drawn.

The shape of the imperfection has been found to play an important role in the buckling behavior. The shape function given in (1) has been shown to be a reliable tool to explain the influence of the shape of the weld imperfection on the buckling behavior. The buckling strength was shown to fluctuate greatly depending on the particular shape of the weld. The roundness of the imperfection at the weld center and the wavelength of the imperfection have been shown to be the governing parameters.

Interaction between neighboring imperfections is an important factor. Strake heights commonly used in silos and tanks do not isolate the effects of circumferential welds on the buckling behavior. Diagrams have been given to determine the weakening effect of this interaction on the buckling strength depending on imperfection amplitude, R/t -ratio, and half-strake height.

Residual stresses are invariably introduced during the welding process and have a strengthening effect on the buckling behavior. Circumferential residual membrane stresses are responsible for this strengthening and can be viewed as internal tension bands around the circumference at the weld. The second contributing factor is the presence of axial stresses and the resulting bending moments. These bending moments can be expected to become relatively more influential in more thick-walled shells and erode the stabilizing effect of the circumferential membrane stresses. Diagrams have been provided to determine the degree of this strengthening effect taking into account variations in R/t -ratio and imperfection amplitude. The strength gain is greater for more thin-walled shells and for smaller imperfection amplitudes.

REFERENCES

- Amazingo, J. C., and Budianski, B. (1972). "Asymptotic formulas for the buckling stresses of axially compressed cylinders with localized or random axisymmetric imperfections." *J. Appl. Mech.*, 93, 179–184.
- Berry, P. A., Rotter, J. M., and Bridge, R. Q. (2000). "Compression tests on cylinders with circumferential weld depressions." *J. Engng. Mech.*, ASCE, 126(4), 405–413.
- Bornscheuer, F. W., Häfner, L., and Ramm, E. (1983). "Zur Stabilität eines Kreiszyllinders mit einer Rundschweissnaht unter Axialbelastung." *Der Stahlbau*, Berlin, 10, 313–318 (in German).
- Calladine, C. R. (1995). "Understanding imperfection-sensitivity in the buckling of thin-walled shells." *Thin-Walled Struct.*, 23, 215–235.
- Ding, X. L. (1992). "Precise engineering surveying—Application to the measurement of large scale steel silos." PhD thesis, School of Civ. and Min. Engrg., University of Sydney, Sydney, Australia.
- Esslinger, M. (1967). "Eine Erklärung des Beulmechanismus von dünnwandigen Kreiszyllinderschalen." *Der Stahlbau*, Berlin, 12, 366–371 (in German).
- Häfner, L. (1982). "Einfluss einer Rundschweissnaht auf die Stabilität und Traglast des axialbelasteten Kreiszyllinders." PhD thesis, Universität Stuttgart, Stuttgart, Germany (in German).
- Hibbit, Karlsson & Sorensen. (1998). *ABAQUS version 5.8-1: Theory manual*, Pawtucket, R.I.
- Holst, F. G., Rotter, J. M., and Calladine, C. R. (1996). "Geometric imperfections and consistent residual stress fields in elastic cylinder buckling under axial compression." *Proc., Imperfections in Metal Silos Workshop, BRITE/EURAM Concerted Action CA-Silos, Working Group 3: Metal Silo Struct.*, 199–216.
- Koiter, W. T. (1945). "The stability of elastic equilibrium." Dissertation, Technische Hooge School, Delft, The Netherlands. English translation by E. Riks: Technical Report AFFDL-TR-70-25, Air Force Flight Dynamics Laboratory, Air Force Systems Command, Wright-Patterson Air Force Base, Ohio, 1970.
- Koiter, W. T. (1963). "The effect of axisymmetric imperfections on the buckling of cylindrical shells under axial compression." *Proc., Kon-*

- inklijke Nederlandse*, Akademie van Wetenschappen, The Netherlands, 66(B), 265–279.
- Pircher, M., Berry, P. A., and Bridge, R. Q. (2000). “The properties of circumferential weld-induced imperfections in silos & tanks.” *Res. Rep. CE17*, CCTR, University of Western Sydney, Sydney, Australia.
- Pircher, M., and Bridge, R. Q. (2000). “Buckling and post-buckling behavior of silos & tanks under axial load—Some new aspects.” *Res. Rep. CE18*, CCTR, University of Western Sydney, Sydney, Australia.
- Ravn-Jensen, K., and Tvergaard, V. (1987). “Effect of residual stresses on plastic buckling of cylindrical shell structures.” *Int. J. Solids Struct.*, Roorkee, India, 26(9–10), 993–1004.
- Rotter, J. M. (1996). “Buckling and collapse in internally pressurised axially compressed silo cylinders with measured axisymmetric imperfections: Imperfections, residual stresses and local collapse.” *Proc., Imperfections in Metal Silos Workshop, BRITE/EURAM Concerted Action CA-Silos, Working Group 3: Metal Silo Structures*, 119–139.
- Rotter, J. M., and Teng, J. G. (1989). “Elastic stability of cylindrical shells with weld depressions.” *J. Struct. Engrg.*, ASCE, 115(5), 1244–1263.
- Steinhardt, O., and Schulz, U. (1970). “Zur Beulstabilität von Kreiszy-linderschalen.” *Bericht der Versuchsanstalt fuer Stahl, Holz, Steine*, Universitaet Karlsruhe, Karlsruhe, Germany.
- Teng, J. G., and Rotter, J. M. (1992). “Linear bifurcation of perfect col-umn-supported cylinders: Support modelling and boundary condition.” *Thin-Walled Struct.*, 14, 241–263.
- Tennyson, R. C., and Muggeridge, D. B. (1969). “Buckling of axisym-metric imperfect circular cylindrical shells under axial compression.” *AIAA J.*, 7(11), 2127–2131.
- White, J. D., and Dwight, J. B. (1977). “Weld shrinkage in large stiffened tubulars.” *Proc., Conf. on Residual Stresses in Welded Constr.*, The Welding Institute, London, 337–348.
- Yamaki, N. (1984). *Elastic stability of circular cylindrical shells*, North-Holland, Amsterdam, The Netherlands.

NOTATION

The following symbols are used in this paper:

- D = elastic axial bending stiffness;
 E = modulus of elasticity;
 L = half-strake height of silo or tank;
 m = number of circumferential buckling waves;
 R = radius of thin-walled cylinder;
 t = wall thickness of thin-walled cylinder;
 w_0 = radial displacement at circumferential weld imperfection;
 x = meridional coordinate measured from weld position;
 ζ = parameter defining degree of roundness at tip of weld;
 λ = half-wavelength of shape of weld imperfection;
 λ_0 = linear meridional bending half-wavelength of thin-walled cylinder [$= \pi \sqrt{Rt/\sqrt{12(1 - \nu^2)}} \approx 2.444 \sqrt{Rt}$];
 ν = Poisson's ratio;
 σ_{cl} = axial buckling stress according to classical theory [$= E \cdot t / (R\sqrt{3(1 - \nu^2)}) \approx 0.605(E \cdot t) / R$];
 σ_{long} = buckling strength of long thin-walled cylinder; and
 σ_{ϕ} = circumferential membrane stress.